Stochastic Optimization For Adaptive Real - Time Wavefront Correction

M. S. Zakynthinaki [*], Y. G. Saridakis [†]
Applied Mathematics & Computers Laboratory
Technical University of Crete
GR 73100 Chania, Crete, GREECE

Abstract

We have investigated the performance of an adaptive optics system subjected to changing atmospheric conditions, under the guidance of the ALOPEX stochastic optimization. Atmospheric distortions are smoothed out by means of a deformable mirror, the shape of which can be altered in order to follow the rapidly changing atmospheric phase fluctuations. In a simulation model, the total intensity of the light measured on a central area of the image (masking area) is used as the cost function for our stochastic optimization algorithm, while the surface of the deformable mirror is approximated by a Zernike polynomial expansion. Atmospheric turbulence is simulated by a number of Kolmogorov filters. The method's effectiveness, that is its ability to follow the motion of the turbulent wavefronts, is studied in detail and as it pertains to the size of the mirror's masking area, to the number of Zernike polynomials used and to the degree of the algorithm's stochasticity in relation to the mean rate of change of atmospheric distortions. Computer simulations and a series of numerical experiments are reported to show the successful implementation of the method.

Keywords: stochastic optimization, ALOPEX algorithm, adaptive wavefront correction, Zernike polynomials, deformable mirror, masking.

AMS (MOS) Classification: 65K10, 78M50, 85A99, 90C15, 90C90, 93B40.

1 Introduction

Atmospheric turbulence causes severe degradations in astronomical images [10, 3, 9, 12]. The main limitations of imaging through the atmosphere are due to the mixing of cold and warm atmospheric layers which results in non-uniformities in the temperature, pressure, density and hence in fluctuations of the refractive index of the atmosphere. The optical effects induced are mainly observed as random intensity fluctuations and random variations in the average position of the centroid of the star under observation. As a result, a typical short exposure image, formed by viewing a point source through turbulence, does not consist of a single diffraction pattern with a diameter fixed by the diffraction limit of the telescope, but rather of a number of superimposed speckles, minute images of the point source, which are distributed over a diameter determined by the severity of turbulence (see Figure 3a).

A deformed wavefront can be corrected by means of the same mechanisms that cause the distortions: adaptive optics systems are designed to cancel out the effects of atmospheric turbulence as well as any other possible sources of optical aberration. Such systems improve

[*]Current address: Departament de Matemática Aplicada I, Universitat Politécnica de Catalunya, Diagonal 647, E-08028 Barcelona, Spain. email:Maria.Zakynthinaki@upc.es

[†]email:yiannis@science.tuc.gr

This work was supported by the Greek General Secretariat of Research & Technology under the grant PENED - 107.527

the spatial resolution of telescope images up to the diffraction limit. By inserting a system that can cause inverse distortions on the image, such a deformable mirror, before the light information gets recorded on the telescope camera, it is possible to cancel out, or at least minimize, the optical effects induced by turbulence. A deformable mirror is able to rapidly alter its shape to the equivalent shape of the wavefront which must be subtracted out [9]. Control of this mirror may be achieved by ordinarily piezo-electric devices (*actuators*), that produce motions of the order of several kHz. These actuators can be driven by an adaptive control algorithm, capable of converting light intensity data into into corrector control signals in a period of time short enough in order that the turbulence has not decorrelated significantly between sensing and correction.

The intensity of light passing through a narrow aperture (*masking area*) on the image plane is used as an objective (*cost*) function in the optimizing algorithm. The suggested control algorithm is the *ALOPEX* stochastic optimization algorithm [2, 11, 3, 8, 9, 12] (see section 3).

The study, among with the simulation of a point source, a telescope system and the distorting atmosphere, investigates

- the typical method's behavior during the process of image restoration
- the optimal size of the masking area
- the system's behavior to the rate of change of the atmospheric distortions
- the optimal algorithm's mean noise amplitude, in relation to the local wind conditions.

Figure 1 shows the optimization cycle: an initial undistorted image of a point star is subjected to phase distortions of the same nature as those that are induced by the turbulent atmospheric layers (see section 2). A correcting phase is then superimposed to the light information via a deformable mirror which is introduced before the image is recorded. The information that is finally measured on the image plane, corresponds only to an area of small aperture around the center of the image (masking area). The total light that passes through this area is evaluated as an indication of image quality. Its value is used as feedback for the ALOPEX optimization, leading to the calculation of the new values of the control variables, through which the new optimal shape of the mirror is evaluated. It should be emphasized that the whole optimization cycle is in phase with, and can follow the rapid changes of the atmospheric conditions.

2 Computer Simulations and Background

Let us assume an image plane (r, ψ) and a telescope aperture (ρ, θ). We have simulated a telescope system, using a modified Fresnel - Kirchhoff integral in a numerical calculation of the image - irradiance distribution $I(r, \psi)$, for monochromatic light and for a point source at infinity [10, 9].

$$I(r,\psi) = \left| \int_0^1 \int_0^{2\pi} e^{ik[\delta(\rho,\theta) - r\rho cos(\theta-\psi)]} \, \rho d\theta d\rho \right|^2 \tag{1}$$

In the absence of the turbulent atmospheric layers, the intensity distribution of a diffraction limited image consists of a central disk, referred to as the *airy disk*, and the surrounding diffraction rings. Figure 2 shows the image of a point star (peak normalized to unity), generated by means of equation 1, assuming that no atmospheric distortion is present.

Before entering the earth's atmosphere the wavefront of a light coming from a point source is essentially flat. The refractive index inhomogeneities within the atmosphere introduce random phase delays into different parts of the wave, resulting in a distorted wavefront. The real

function $\delta(\rho,\theta)$ in equation 1 includes the optical effects of both the distorting atmosphere $\phi(\rho,\theta)$ and the correcting mirror $\phi_c(\rho,\theta)$,

$$\delta(\rho,\theta) = \phi(\rho,\theta) - \phi_c(\rho,\theta) \ . \tag{2}$$

It is worth noticing that the undistorted image of the point source, shown in Figure 2, corresponds to $\delta(\rho,\theta) = 0$. The correcting phase can be approximated by use of a Zernike polynomial expansion,

$$\phi_c(\rho,\theta) \approx \sum_{j=1}^{N} a_j Z_j(\rho,\theta) \ , \qquad \Delta_N \approx 0.2944 \ N^{\frac{-\sqrt{3}}{2}} \left(\frac{D}{r_0}\right)^{\frac{5}{3}} [rad^2] \ , \tag{3}$$

where Δ_N denotes the error in an approximation of N Zernike polynomials (for $N > 10$), D is the telescope aperture and r_0 is the correlation lenght, known as the Fried parameter [1], corresponding to areas of nearly constant atmospheric distortion. For a more detailed description of Zernike polynomials see [7, 9, 12].

The behavior of the atmospherically distorted wavefront at the telescope pupil is modeled in terms of Kolmogorov theory [4], which predicts the statistical properties of the refractive index fluctuations and leads to equations which describe the turbulence induced by the thin layers within the atmosphere. To simulate the atmospheric distortion we introduced a phase screen, i.e. a two dimensional distribution of phase fluctuations, satisfying a Kolmogorov spectrum, into the optical system and at each iteration of the optimizing algorithm (recall Figure 1). Atmospheric phase variations are numerically generated [5, 9] by the so - called *Random mid - point displacement* algorithm, used for the same purposes by Lane et al [5], and is transported across the telescope aperture according to local wind conditions.

As predicted by Kolmogorov theory, the phase fluctuations cause the image formed by a large telescope to break up into a number of speckles. Figure 3a shows a sample of simulated speckled images, produced by the introduction of the turbulent phase screen into the simulated telescope system. Such a speckle pattern fluctuates rapidly as the refractive index distribution changes. Due to random motion and random shape fluctuations of the speckle pattern, the image that is finally recorded on the telescope camera, is, as a superposition of speckles, an image of large angular extend, typically looking like the one shown in Figures 3b and 3c, where a spreading of the point source image is observed, a well as a considerable decrease of the central intensity (peak) of the light distribution. Figures 3b and 3c correspond to a superposition of 1000 speckled images, like the one shown in Figure 3a. They present a typical long exposure image.

The restoration process has as input the total light information that passes, at every time step, through the masking area. Assuming a central masking area of diameter R, the light recorded inside this area can be represented by the integral

$$S \equiv \int_{-R}^{R} \int_{0}^{2\pi} I(r,\psi) \ r d\psi dr \ , \tag{4}$$

which can be used to evaluate the cost function S that describes the simulated system.

For an evaluation of the image quality obtained, the *Strehl Ratio - SR* is defined as a restoration criterion, to estimate the sharpness of the restored images, as $SR = \frac{I(0)}{M(0)}$, where $M(r)$ is the irradiance distribution of the undistorted image.

3 Stochastic optimization

For the purpose of optimization, let $f(x_1, x_2, ..., x_N)$ denote the *cost function*, that is the function that describes the system, which depends on a group of the N parameters $x_1, x_2, ..., x_N$, called the *control variables* of the system. The stochastic optimization algorithm used for the maximization of the cost function f is the so-called ALOPEX (*ALgorithm Of Pattern*

EXtraction), and was originally devised in [2, 11] for the purpose of experimentally determining receptive fields of individual neurons in the visual pathway. The ALOPEX optimization method was modified [3, 8, 9, 12] and new versions were introduced and studied, among with the ones already known. The cost function that describes our system is the function $f(x_1, x_2, ..., x_N) \equiv S(a_1, a_2, ..., a_N)$, defined by equation 4. Recalling equations 1, 2, 3 and 4, it is easy to see that S is a function of the N variables $a_1, a_2, ..., a_N$ that determine the correcting phase and thus shape of the deformable mirror.

ALOPEX process operates as follows: Let $S^{(n)}({a_1}^{(n)}, {a_2}^{(n)}, ..., {a_N}^{(n)})$ be the value of the cost function at the n-th iteration and let ${a_i}^{(n)}$ be the value of the i-th control variable at the n-th iteration. According to the version of the ALOPEX stochastic optimization algorithm presented below [8], the value of the i-th control variable is evaluated, at each iteration, according to the rule:

$$a_i^{(n)} = a_i^{(n-1)} + c\Delta {a_i}^{(n-1)} \frac{\Delta S^{(n-1)}}{\mid \Delta S^{(n-2)} \mid} + g_i^{(n)} \quad , \quad n = 1, 2, \dots \quad , \quad i = 1, \cdots, N \tag{5}$$

where $\Delta a_i^{(n)} = {a_i}^{(n)} - {a_i}^{(n-1)}$ and $\Delta S^{(n)} = S^{(n)} - S^{(n-1)}$. The needed initial values of $a_i^{(n)}$, $n = -2, -1, 0$ are computed randomly while their corresponding values of $S^{(n)}$, $n = -2, -1, 0$ are computed by making use of equations (1)-(4). The noise terms g_i are essential ingredients in the process [2, 11, 3, 8, 9, 12], as they provide the agitation necessary to drive the process and to overcome local extrema. The dynamics of the process depends strongly on the amplitude and the frequency spectrum of the g_i terms.

With use of the above version of the ALOPEX stochastic optimization algorithm, the value of the characteristic constant c remains unchanged all during the optimization process. For the results presented in the present paper, the value of c was kept constant to $c = 0.4$.

For a more detailed discussion on the above version of ALOPEX algorithm, see [8, 12].

4 Numerical Experimentations

4.1 Image Restoration and the Size of the Masking Area

The results presented in Figures 4 correspond to a detailed study of the simulated telescope system, during an optimization process of duration of 1000 time steps and when $N = 6$ Zernike polynomials are used to describe the correcting surface. For the understanding of the data shown in Figures 4, we define the parameters: μ = (masking area diameter)/(airy disk diameter), $\mu_1 \equiv \frac{D_m^{restored}}{D_m^{distorted}}$, and $\mu_2 \equiv \frac{SR\ restored\ image}{SR\ distorted\ image}$, where D_m is the diameter of the light distribution at half its maximum (otherwise known as FWHM - *Full Width at Half Maximum*). Recall that the airy disk is the central disk of the intensity distribution of the point source (see Figure 2).

As observed from Figures 4 the optimal masking area diameter is close to the diameter of the airy disk of the point source. In particular, best results were obtained for $\mu = 1.25$. Figure 5 shows a representative restored image, for a correcting phase of $N = 6$ Zernike polynomial and $\mu = 1.25$ (recall Figure 3 in which the initial distorted image is presented). The exposure time in Figure 5, as well as in Figure 3, was 1000 time steps. The mean noise amplitude was kept equal to $< g_i >= 0.924 \cdot 10^{-2}\ D_{speckles}$, where $D_{speckles}$ is the average diameter of the speckle pattern (obviously the parameter $D_{speckles}$ depends strongly on the severity of the turbulence). This mean value of noise amplitude was considered to be the optimal, as it pertains to the successful implementation of the restoration process, and the speed of convergence (see sections below).

We will now describe the process of image sharpness restoration. Assuming that the centroid of an image is the center of gravity of its intensity distribution, the optimizing method

aims at its re-centering, in real time. With help of the deformable mirror, an optimization of the light distribution of the image is achieved as well.

Figure 6 presents a snapshot of an image as it would have been recorded on the telescope camera, (a) without the optimization (speckles) and (b) with the optimizing system turned on. For the optimization shown in Figure 6, the number of variables (number of Zernike polynomials used in the expansion) was kept equal to $N = 6$, and the diameter of the mask R was kept constant and equal to 1.25 times the diameter of the source's airy disk. It is easy to observe that, although turbulence tends to move the centroid of the speckles outside the central masking area (Figure 6a), the optimizing process with help of ALOPEX algorithm manages to follow this movement, while at the same time successfully restore the sharpness of the image (Figure 6b).
We note that Figures 6 correspond to the $\frac{1}{1000}$ of the exposure time of Figure 5: the sample of a restored image, shown in Figure 5 represents a superposition of 1000 restored speckled images, like the ones shown in Figures 6.

4.2 Image Restoration and the Number of Zernike Polynomials

The following section presents the study of the behavior of the optimizing method when the degree of freedom of the correcting surface, i.e. the number of Zernike polynomials used in the expansion of equation 3 which describes the correcting phase, is no more constant. It is worth noticing that, if N is the number of Zernike polynomials, the number of variables controlling the mirror's surface is $N - 1$ (the first Zernike polynomial is a constant defining the mirror's position in space; its role is not important to the behavior of the optimizing process, see [7, 9]).

For the statistical results shown in Figure 7, which correspond to an exposure time of 1000 time steps, the ratio of the masking area diameter to the diameter of the airy disk was kept equal to $\mu = 1.25$. For all the numerical experiments, the initial condition of a perfectly aligned flat mirror was kept the same.

It is worth adding that, for optimal convergence, the mean noise amplitude is constant and only varies when the number of Zernike polynomials changes. So there is: $< g_i >= 1.964 \cdot 10^{-2}\ D_{speckles}$, for $N = 3$ Zernike polynomials, $< g_i >= 0.924 \cdot 10^{-2}\ D_{speckles}$ for $N = 6$, $< g_i >= 0.628 \cdot 10^{-2}\ D_{speckles}$ for $N = 10$, $< g_i >= 0.524 \cdot 10^{-2}\ D_{speckles}$ for $N = 15$ and $< g_i >= 0.267 \cdot 10^{-2}\ D_{speckles}$ for $N = 21$ Zernike polynomials.

4.3 Image Velocity and the Noise of the Stochastic Process

4.3.1 Image restoration versus the mean velocity of speckles

The study of the simulated adaptive system will be completed with the investigation of the method's behavior to the rate of change of the position of the centroid of speckles and the shape of the speckle pattern, which is directly related to the rate of change of the turbulent profile. It is worth noticing that, although atmospheric conditions vary according to the wind, reference to specific wind velocities has no practical meaning, as speed in the atmosphere varies according to height. Hence, a measure of the wind velocity is not sufficient to describe the rate of change of the atmospheric conditions. It is thus necessary to assume a different quantity for the description of the speed, with which the distortion imposed on the light information changes: assuming short time intervals Δt of the order of a few time steps, corresponding to times shorter than the correlation time of the turbulence, we can calculate a mean value of the rate of change of the position of the centroid of the speckles, $\bar{v}_{speckles}$. The mean velocity of speckles is expressed in terms of the diameter of the circular telescope aperture D and in units of $D/(time\ step)$. It should be noted that the distortion a correcting system has to deal with, is not restricted to the effects of the atmospheric turbulent conditions but is extended to the compensation of other parameters as well, such as thermal effects within the enclosure and above the surface of the mirror, distortions in the telescope optics, or other possible external

factors. In the present simulated model, the system with help of the ALOPEX algorithm is called to cancel out a phase $\phi(\rho, \theta)$ which corresponds to the overall distortion imposed on the light information. Using units of $D/(time\ step)$ as a measure of the mean image velocity, the image movement is described with no reference to a specific source of distortion.

The image restoration process was studied for various rates of change of the distortion. For the results presented in Figures 8, the mean distortion velocity $\bar{v}_{speckles}$ varies from $3.003 \cdot 10^{-4}$ to $61.225 \cdot 10^{-4} D/(time\ step)$, while the mean noise amplitude is constant and only changes when the number of Zernike polynomial change, as presented in the previous paragraph. It is easy to observe that a constant mean noise amplitude fails to satisfactory restore the image, when the image velocity is large (see Figure 8). For mean image velocities larger than $\bar{v}_{speckles} > 24.194 \cdot 10^{-4}$ the final image sharpness is no more the optimal. Recall that for an estimation of the image quality obtained, the parameters $\mu_1 \equiv \frac{D_m^{restored}}{D_m^{distorted}}$ and $\mu_2 \equiv \frac{SR\ restored\ image}{SR\ distorted\ image}$ are defined.

We expect that this limiting behavior of the restoration process will be successfully overcome by the appropriate choice of the algorithm's parameters. Indeed, as shown in the paragraph that follows, it is necessary to implement different degrees of stochasticity, i.e. different mean noise amplitudes $< g_i >$ to reach satisfactory performance.

4.3.2 Image restoration versus noise amplitude

Figures 9 and 10 summarize the results of a study of the method's behavior when the mean noise amplitude $< g_i >$ follows the changes in the mean image velocity. We note that the $< g_i >$'s are kept constant up to a mean speckle velocity of $\bar{v}_{speckles} = 20.013 \cdot 10^{-4}\ D/(time\ step)$, due to their successful implementation (see section above). Above this limit the optimal $< g_i >$'s are found by trial and error.

Figure 9 gives an estimation of the optimal mean noise amplitude $< g_i >$ for different values of the mean image velocity and for the different degrees of freedom, $N = 6$, $N = 10$, $N = 15$ and $N = 21$. It is easy to see that the system's behavior is very sensitive to the choice of the degree of stochasticity and the mean noise amplitude needed for optimal results is almost linearly related to the mean speckle velocity. More specifically, a least square approximation can be found for the relation of the $< g_i >$'s and $\bar{v}_{speckles}$: There yields, $< g_i >= 0.246 \cdot \bar{v}_{speckles} + 0.919 \cdot 10^{-2}$ for $N = 6$, $< g_i >= 0.202 \cdot \bar{v}_{speckles} + 0.588 \cdot 10^{-2}$ for $N = 10$, $< g_i >= 0.096 \cdot \bar{v}_{speckles} + 0.521 \cdot 10^{-2}$ for $N = 15$ and $< g_i >= 0.152 \cdot \bar{v}_{speckles} + 0.248 \cdot 10^{-2}$ for $N = 21$.

Figures 10 present the intensity spread restoration and the accomplished values of the SR (parameters μ_1 and μ_2 respectively). It is shown how the appropriate change in the algorithm's mean noise amplitude (see Figure 9), under change in the rate of change of the atmospheric conditions, affects the system's behavior (compare Figures 8).

5 Conclusion

We summarize the main results as follows:

- The optimal value of the diameter of the system's masking area is close to the diameter to the point source's airy disk.
- A correcting phase represented by an approximation of 6 Zernike polynomials is able to satisfactory represent a distorted wavefront.
- The degree of stochasticity of the optimization algorithm is directly related to the rate of change of the atmospheric conditions.

- The mean noise amplitude of the optimization algorithm has to be decreased, as the number of Zernike polynomials used for the approximation of the correcting phase is increased.

Also, observe that our approach is characterized by:

- its easy and cost effective implementation by analog networks,
- no interferometry is required, making this method applicable to even weak sources, and at the same time greatly reducing the complexity and cost of the system,
- no knowledge of the dynamics of the system, or of the functional dependence of the cost function on the control variables, is required,
- the system can be conveniently employed within existing telescopes.

As a final remark we would like to point out that, in such a demanding application, our relatively simple to implement approach is extremely competitive.

References

[1] Fried, D. L., *Statistics of a Geometric Representation of Wavefront Distortion* Journal of the optical society of America, vol.55, November 1965

[2] Harth, E., Tzanakou, E., *Alopex: A stochastic method for determining visual receptive fields* Vision Research, 14, 1475-1482, 1974.

[3] Kalogeropoulos, T. E., Saridakis, Y. G., Zakynthinaki, M. S., *Improved Stochastic Optimization Algorithms for Adaptive Optics*, Computer Physics Communications, 99 (1997), 255-269.

[4] Kolmogorov A. N., *Turbulence* S.K.Friedlander, L.Topper (Eds.), Interscience, NY 1965

[5] Lane, R. G., Glindemann, A., Dainty, J. C., *Simulation of a Kolmogorov phase screen*, Waves in random media, 2, 209-224, 1992.

[6] Lena, P., Lebrun, F., Mignard, F., *Observational astrophysics* 2nd ed., Springer-Verlag, Berlin, 1996.

[7] Noll, R. J., *Zernike Polynomials and Atmospheric Turbulence* Journal of the optical society of America, Vol.66, 3 March 1976

[8] Saridakis, Y. G., Zakynthinaki, M. S., *Towards the Improvement of the ALOPEX II Stochastic Optimization Algorithm*, Proc. of the third Hellenic-European conference on mathematics and informatics (HERMES), September 26-28, 1996-Athens, LEA ed., p.251-258

[9] Saridakis, Y. G., Zakynthinaki, M. S., Kalogeropoulos, T.E., *Wavefront Correction by use of Zernike polynomials and ALOPEX stochastic optimization*, International Journal of Applied Science and Computation, vol.5, no.3, February 1999, pp.252-274.

[10] Tyson, R. K., *Principles of Adaptive Optics* Academic Press, 1991

[11] Tzanakou, T., Michalak, R., Harth, E., *The Alopex Process: Visual Receptive Fields by Response Feedback* Biological Gybernetics, 35, 161-174, 1979.

[12] M. Zakynthinaki, *Stochastic optimization for adaptive correction of atmospheric distortions in astronomical observation* PhD thesis (in Greek), Technical University of Crete, June 2001.

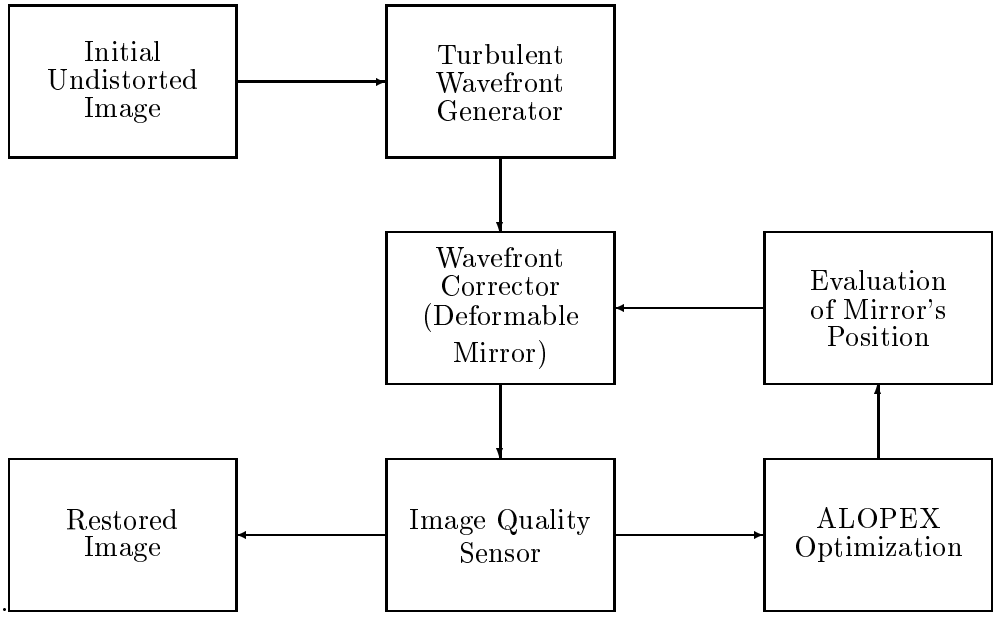

Figure 1: The simulated Adaptive Optics system

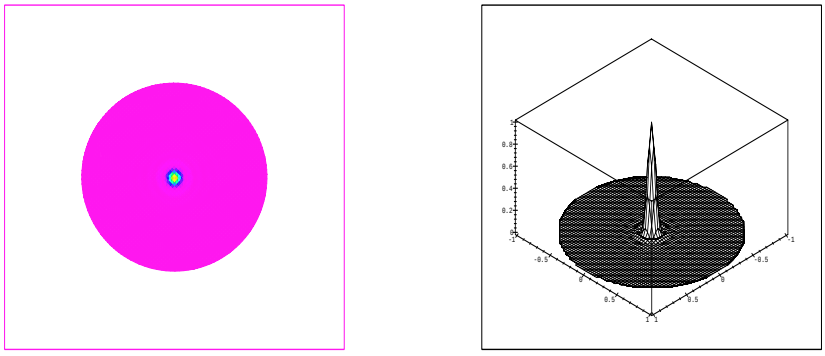

a. b.

Figure 2: The image of a point star - no disturbing atmosphere is present, (a) as shown on the image plane and (b) irradiance distribution

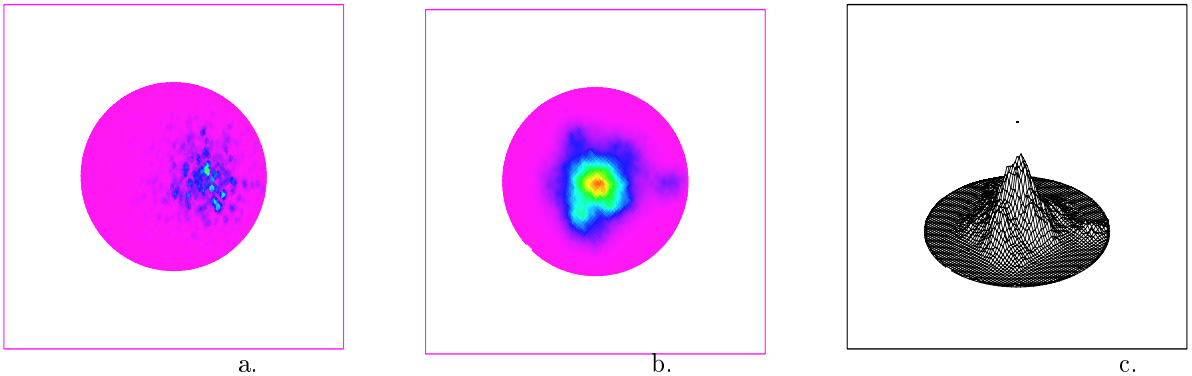

a. b. c.

Figure 3: A distorted image, (a) speckle sample, (b) long exposure image, as shown on the image plane and (c) irradiance distribution of a (b)

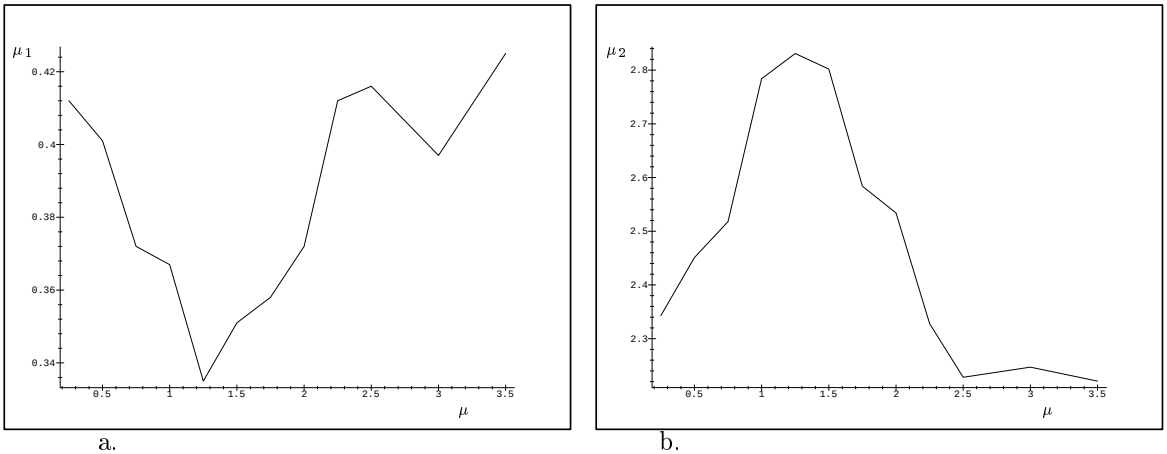

a. b.

Figure 4: (a) Intensity spread restoration and (b) SR restoration versus the diameter of the masking area

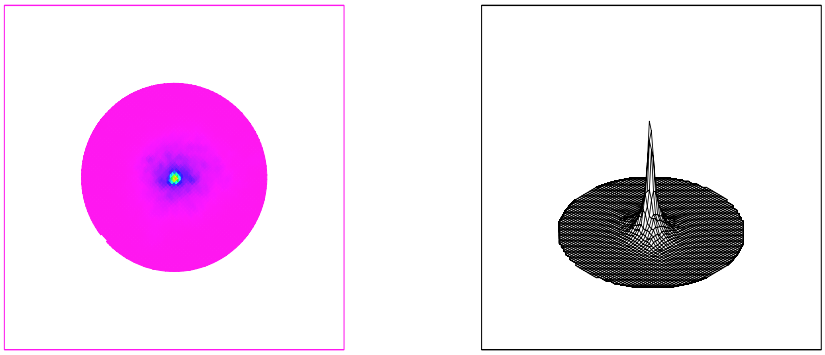

a. b.

Figure 5: Sample of a restored image - $N = 6$. (a) as shown on the image plane, (b) irradiance distribution

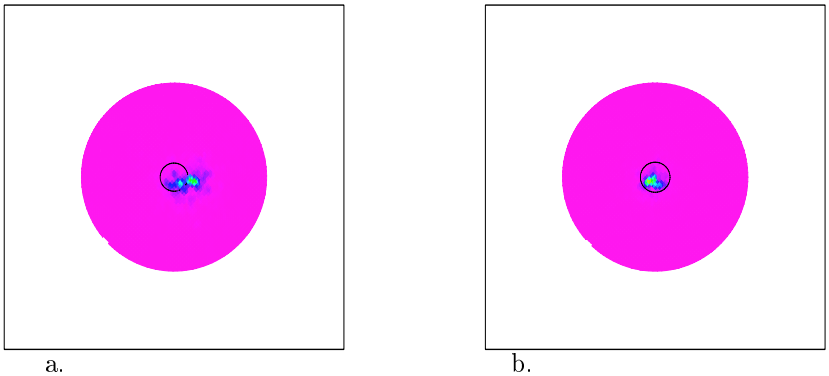

a. b.

Figure 6: Restoration of the speckled image. ALOPEX algorithm (a) off and (b) on.

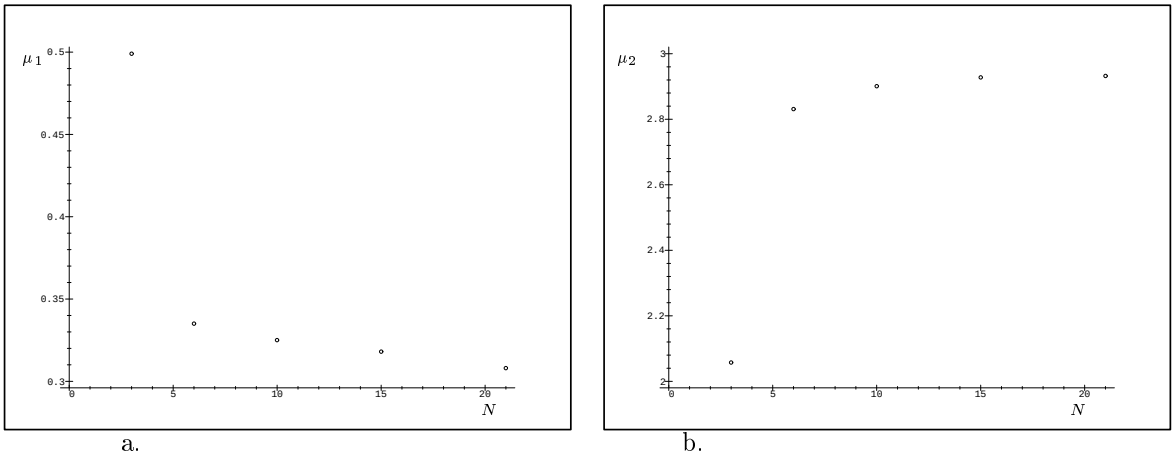

a. b.

Figure 7: (a) Intensity spread restoration and (b) SR restoration versus the number of Zernike polynomials

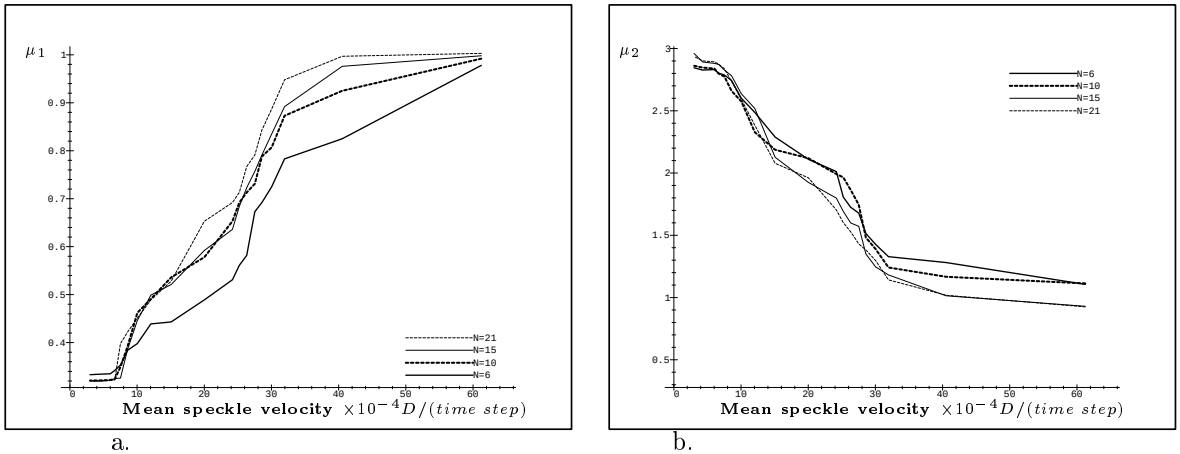

a. b.

Figure 8: (a) Intensity spread restoration and (b) SR restoration versus mean speckle velocity - Constant mean noise amplitude

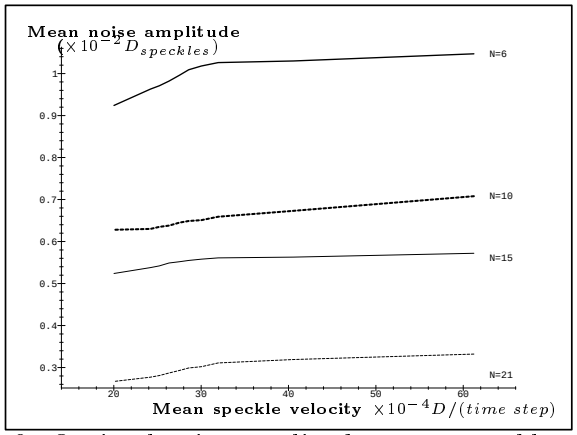

Figure 9: Optimal noise amplitude versus speckle velocity

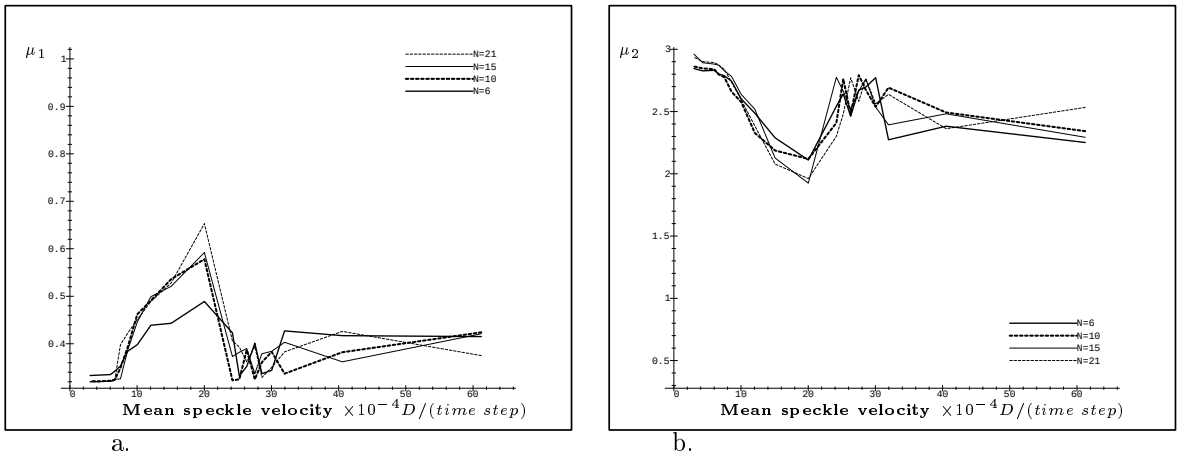

a. b.

Figure 10: (a) Intensity spread restoration and (b) SR restoration versus mean speckle velocity - Changing mean noise amplitude